JUSAN SCIENCE

Journal of Engineering and Environmental Systems

ISSN (Print): 3135-2510; ISSN (Online): 3135-2529

journal homepage: https://jusanscience.com/journals/jees

Research Article

Integrated Geospatial and Statistical Modeling of Potentially Toxic Elements in Soils of the Temirtau Industrial Area, Kazakhstan

Yryszhan Zhakypbek[1], Miras Amirkhanov[1*], Yerkezhan Begimzhanova[2*], Ardana Aben[1], Ayaulym Toishy[1], Yelaman Abdalimov[1]

[1]Mining and Metallurgical Institute named after O. A. Baikonurov, Satbayev University, 22 Satbayev Street, Almaty 050013, Kazakhstan.

[2]Center for Remote Sensing and GIS "Terra" LLP, 83 Roza Baglanova Street, Almaty 050010, Kazakhstan.

Corresponding authors: mirasamirkhanov@gmail.com; yerkezhan.bg@gmail.com

https://doi.org/10.66973/jees.26.012

Article info:

Received: 22 September 2026 / Revised: 03 November 2026 / Accepted: 20 November 2026 / Published: 25 November 2026

Y. Zhakypbek, M. Amirkhanov, Y. Begimzhanova, A. Aben, A. Toishy, and Y. Abdalimov, "Integrated geospatial and statistical modeling of potentially toxic elements in soils of the Temirtau industrial area, Kazakhstan," Journal of Engineering and Environmental Systems, 2, 169-183. https://doi.org/10.66973/jees.26.012

Abstract: This study investigated the spatial distribution and statistical relationships of nine potentially toxic elements (As, Pb, Zn, Cu, Ni, Co, Mn, Cr, and Ba) in surface soils of the Temirtau industrial area, Kazakhstan. Twenty-five soil samples (0–15 cm) collected in 2024 were analyzed using X-ray fluorescence spectrometry. Ordinary kriging, distance-based analysis, Pearson correlation, regression modeling, and ArcGIS-based raster integration were employed. Spatial interpolation revealed relatively elevated concentrations of Pb, Zn, Cu, Mn, Ba, and Cr near industrial facilities, whereas As, Ni, and Co exhibited more dispersed distributions. The strongest reported correlation was observed between Mn and Cu ($r = 0.64$, $p = 0.0005$). A cubic regression model for Zn–Cr yielded an in-sample R^2 of 0.79, although alternative models showed lower approximation errors. The mapped area of industrial waste deposits increased from 38 ha in 1985 to 96 ha in 2024, representing a 2.53-fold expansion. These findings highlight spatial heterogeneity and inter-element associations, providing a basis for targeted environmental monitoring. However, limitations in analytical quality control, interpolation validation, and model assessment restrict the predictive reliability and environmental risk interpretation of the results.

Keywords: *potentially toxic elements; soil contamination; ordinary kriging; regression analysis; geospatial modeling; Temirtau; industrial pollution.*

1 Introduction

Soil contamination by potentially toxic elements (PTEs) is a major environmental concern associated with industrial development. Studies have documented heavy metals in soybean grains [1] and potential ecological risks from hazardous elements in urban soils [2]. Related research on desertification in

© 2026 Jusan Science Publisher LTD. All rights reserved.
This is an open access article distributed under the terms of the Creative Commons Attribution (CC BY 4.0) license.

Kazakhstan highlights the broader challenge of managing degraded landscapes [3]. Metallurgical, mining, and energy-production activities can release PTEs, which may persist and accumulate in soils. Integrated GIS and multivariate statistical approaches have been reviewed for assessing regional heavy-metal contamination [4]. In the Karaganda industrial region, investigations have reported heavy-metal accumulation and technogenic pollution of urban soils [5], [6], [7]. These findings emphasize the need for systematic soil monitoring. Lead (Pb), zinc (Zn), copper (Cu), manganese (Mn), chromium (Cr), nickel (Ni), cobalt (Co), arsenic (As), and barium (Ba) exhibit different geochemical behavior. Their distributions can vary with emission sources, atmospheric transport, terrain, and soil properties, as illustrated by studies of anthropogenic metal pollution, soil–plant systems, and contaminated dust [8], [9], [10]. Investigations near mine tailings and lead–zinc processing facilities also demonstrate heterogeneous element accumulation [11], [12], [13].

Metal-contamination assessments spanning mine-related soils, sediments, water bodies, and adjacent ecosystems demonstrate the importance of spatial sampling [14], [15]. Studies in industrial districts and lead–zinc mining regions have characterized trace-element distributions and investigated possible sources [16], [17]. Related investigations of mining-affected soils, rivers, and cultivated land illustrate that contamination varies across environmental settings [18], [19], [20]. GIS, remote sensing, and geostatistical methods can help visualize such spatial variability, but mapped concentrations alone cannot establish shared emission sources or causal pathways.

Positive matrix factorization has been applied to investigate candidate sources of soil metals around lead–zinc tailings [21]. Research on ecological restoration and land-management strategies addresses the related challenge of rehabilitating mining-affected landscapes [22], [23], [24]. Studies of contaminated catchments, soil-forming substrates, GIS–statistical integration, and multivariate source assessment provide complementary approaches to mapping and interpreting soil metals [25], [26], [27], [28]. Kriging-based assessment of soil organic pollutants [29] and spatial analysis of coastal oil contamination [30] are methodological examples, rather than direct evidence of metal pollution in Temirtau. The Temirtau industrial area in Central Kazakhstan contains metallurgical facilities and waste-storage areas that have been examined using remote-sensing observations [31]. These conditions motivate an examination of soil PTE distributions and associations in the present study.

This study aimed to characterize the spatial distribution and statistical relationships of nine PTEs (As, Pb, Zn, Cu, Ni, Co, Mn, Cr, and Ba) in soils from the Temirtau industrial area. The objectives were to (1) map element concentrations using geostatistical interpolation; (2) examine spatial patterns in relation to industrial facilities and selected environmental variables; (3) quantify pairwise associations using Pearson correlation analysis; and (4) compare regression models for selected element pairs.

❖

2 Materials and methods

2.1 Study Area

The study was conducted in the industrial area of Temirtau, Karaganda Region, Central Kazakhstan. The area includes metallurgical facilities, associated industrial infrastructure, and industrial waste-storage sites that may contribute to PTE accumulation in nearby soils [31]. Mercury has also been reported in soils and deposits of the Nura River floodplain in Central Kazakhstan [32], although that earlier study concerns a different element and does not establish contamination at the present sampling points.

Field sampling was conducted in 2024. In total, 25 surface-soil samples were collected from the 0–15 cm layer. Sampling locations were chosen with consideration of their proximity to industrial facilities and anticipated anthropogenic influence; therefore, the available description does not establish that sampling was random or spatially representative of the entire area. GPS coordinates were recorded and imported into the GIS.

2.2 Laboratory Analysis

Concentrations of arsenic (As), lead (Pb), zinc (Zn), copper (Cu), nickel (Ni), cobalt (Co), manganese (Mn), chromium (Cr), and barium (Ba) were measured using a Rigaku NEX CG II X-ray fluorescence (XRF) spectrometer. The reported concentrations were subsequently used for the statistical and spatial analyses. The manuscript does not document analytical uncertainty or quality-control results; consequently, measurement reliability cannot be independently assessed from the information provided.

2.3 Geospatial Analysis and Spatial Interpolation

Ordinary kriging was used in ArcGIS to interpolate the concentration of each element separately. Multivariate statistical and GIS methods have previously been combined to investigate potential

© 2026 Jusan Science Publisher LTD. All rights reserved.
This is an open access article distributed under the terms of the Creative Commons Attribution (CC BY 4.0) license.

sources of soil metals [33]. The spatial-correlation principles underpinning kriging are established in geostatistical methodology [34], while comparisons of interpolation methods emphasize the need to assess accuracy and uncertainty [35]. Distance-based buffer analysis considered distances of 1–13 km from industrial facilities; the Methods state that mean concentrations were calculated by distance interval, although these means are not displayed in the Results. Terrain slope, the normalized difference vegetation index (NDVI), soil nitrogen content, and soil organic carbon were also represented as spatial layers. Here interpolation remains exploratory because variogram fitting, spatial resolution, cross-validation, and prediction uncertainty were not reported.

2.4 Integrated Spatial Modeling

ArcGIS ModelBuilder was used to combine reclassified element-concentration rasters with selected environmental and anthropogenic layers using the Reclassify and Weighted Sum tools. Integrated geospatial indicators have also been used in regional land-degradation assessment [36], but this precedent does not validate the present metal maps. Soil variables are potentially relevant because metal retention depends on mineral–organic interfaces and chemical speciation [37], [38], and mobility may vary with pH and dissolved organic carbon [39]. The original Methods describe equal weights, whereas the Results describe weights based on correlations; these accounts require clarification. Nine element-specific integrated maps were generated. Without the actual layer weights, transformations, and validation, these outputs should be treated as exploratory composite spatial indicators, not measured concentrations, calibrated probabilities, or forecasts. Figure 1 outlines the reported workflow.

2.5 Statistical Analysis

For each pair of measured elements, Pearson's correlation coefficient was used to summarize the linear association across sampling locations. The sample correlation coefficient is defined as:

$$r = \frac{\sum_{i-1}^{n}(X_i-\bar{X})(Y_i-\bar{Y})}{\sqrt{\sum_{i-1}^{n}(X_i-\bar{X})^2}\cdot\sqrt{\sum_{i-1}^{n}(Y_i-\bar{Y})^2}} \quad (1)$$

Here x_i and y_i are the measured concentrations of the two elements at sampling location i; $\bar{x}$ and $\bar{y}$ are their respective sample means; and n is the number of paired observations (nominally 25). The reported p-values were not independently recalculated because the underlying dataset was unavailable.

Linear, quadratic, cubic, power-law, logarithmic, and exponential regressions were compared for selected element pairs. Comparisons of regression and tree-based approaches have been reported for soil cadmium assessment [40], illustrating the importance of evaluating alternative model structures. The present manuscript reports R^2 and a 'mean approximation error (%)' for each fit, but does not define the latter statistic or the selection rule. The conventional in-sample coefficient of determination, for models fitted on the original response scale, is:

$$R^2 = \sqrt{1 - \frac{\sum(y_i-\hat{y}_i)^2}{\sum(y_i-\bar{y}_i)^2}} \quad (2)$$

Here y_i is an observed response, $\hat{y}_i$ is its fitted value, and $\bar{y}$ is the mean observed response. R^2 quantifies in-sample fit; a higher R^2 does not, by itself, demonstrate predictive accuracy or a physically meaningful nonlinear mechanism.

The statistical software, parameter-estimation methods, and treatment of transformed response variables were not specified. No residual diagnostics, adjusted R^2, information criteria, or out-of-sample errors were provided. Accordingly, the regressions are presented as descriptive fits, not independently validated models. The GIS workflow includes distance from industrial sources, terrain slope, NDVI, soil pH, nitrogen content, and soil organic carbon, with possible use of inter-element correlations. Because the weighting scheme is not specified consistently or validated, these layers cannot establish the relative causal importance of individual factors.

© 2026 Jusan Science Publisher LTD. All rights reserved.
This is an open access article distributed under the terms of the Creative Commons Attribution (CC BY 4.0) license.

https://doi.org/10.66973/jees.26.012

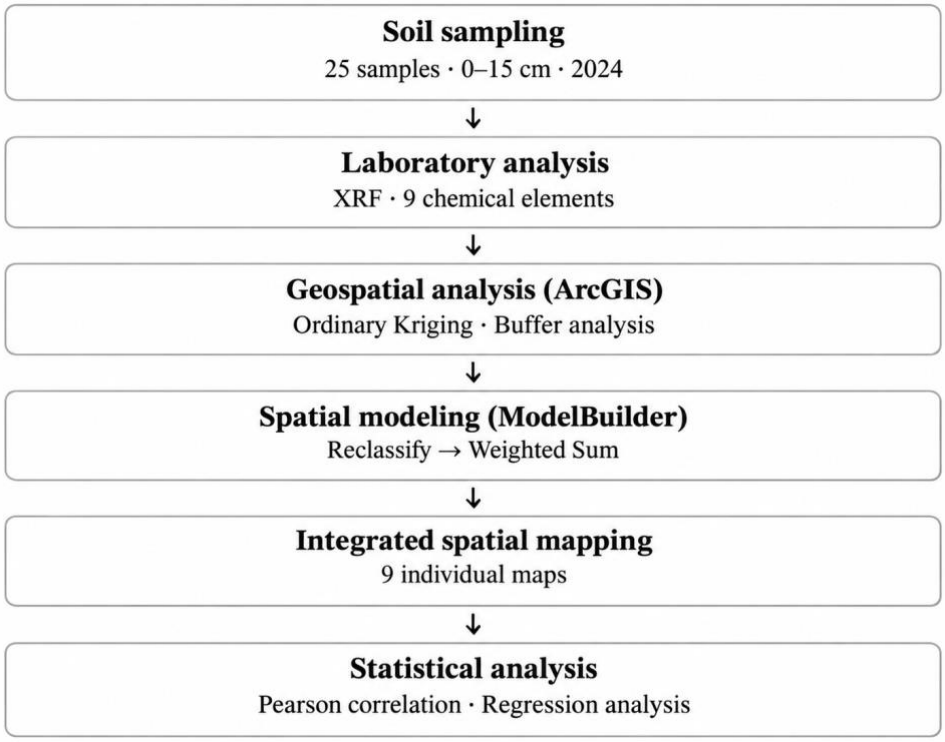

Figure 1. Workflow for soil sampling, elemental analysis, geospatial processing, integrated mapping, and statistical analysis.

3 Result and discussion

The interpolated concentration surfaces indicate spatial variability among the nine measured elements in the Temirtau study area. A meta-analysis has examined the distribution and potential risks of PTEs in soils near coal-industrial sites [41], and air-quality data have been investigated as predictors for spatial soil-metal mapping in an oil-mining region [42]. These studies provide context for possible industrial influences, but the available Temirtau data cannot quantify individual sources or transport pathways. Results are therefore described as mapped concentration patterns, reported distance associations, inter-element correlations, regression fits, and composite GIS indicators. The maps require caution because only 25 sampling locations were included and interpolation validation was not reported.

Ordinary-kriging maps (Figure 2) suggested localized areas of relatively elevated Pb, Zn, Cu, Mn, Ba, and Cr concentrations near industrial facilities and waste-storage sites. Some mapped zones overlap spatially, but overlapping interpolated surfaces are not independent evidence of shared emission sources. The manuscript does not provide a complete concentration summary, local geochemical background, or comparison with regulatory thresholds; therefore, these areas should not be designated as contaminated or hazardous solely on the basis of the maps.

In contrast, the interpolated distributions of As, Ni, and Co were more dispersed, with elevated values appearing at several locations across the study area. Field monitoring and Pb-isotope analysis have linked atmospheric deposition with soil-metal accumulation [43], while separate work has examined the mobility of trace elements in Zn–Pb metallurgical dust [44]. Such pathways may be relevant for hypothesis generation but were not directly measured or isolated in this study.

The observed patterns are descriptive and conditional on the sampling layout and interpolation assumptions. Without cross-validation and uncertainty maps, it is not possible to determine the accuracy of predicted concentrations between sampling locations. Additional strategically placed samples would be needed to evaluate the apparent hotspots and assess their extent.

© 2026 Jusan Science Publisher LTD. All rights reserved.
This is an open access article distributed under the terms of the Creative Commons Attribution (CC BY 4.0) license.

https://doi.org/10.66973/jees.26.012

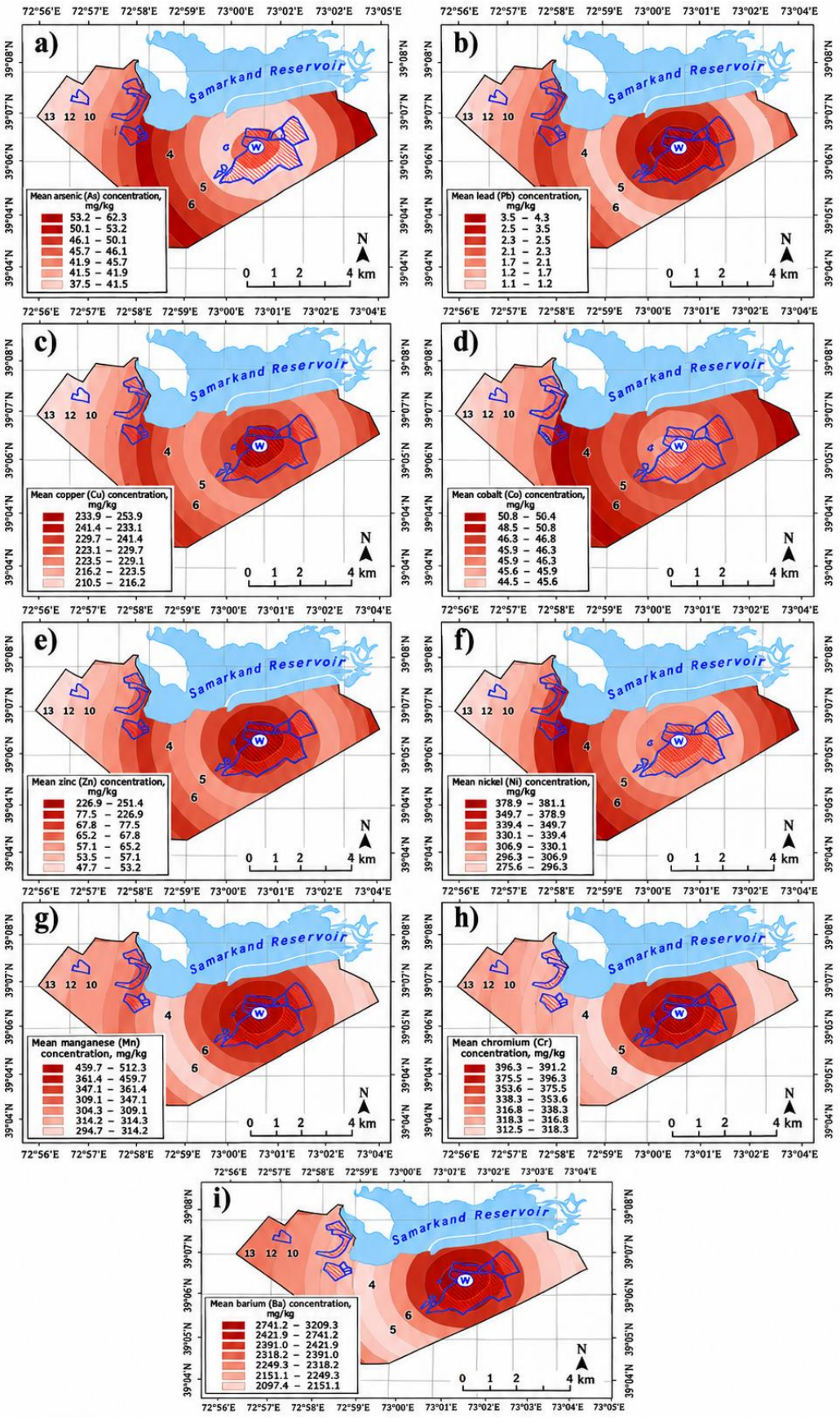

Figure 2. Interpolated spatial distributions of nine potentially toxic elements in the Temirtau industrial area: (a) As; (b) Pb; (c) Cu; (d) Co; (e) Zn; (f) Ni; (g) Mn; (h) Cr; and (i) Ba.

© 2026 Jusan Science Publisher LTD. All rights reserved.
This is an open access article distributed under the terms of the Creative Commons Attribution (CC BY 4.0) license.

https://doi.org/10.66973/jees.26.012

Figure 3 displays negative associations between distance from industrial facilities and the measured element concentrations, with different magnitudes across elements. It is a plot of correlation coefficients, not the mean concentrations for the 1–13 km buffer intervals described in the Methods. Therefore, it does not establish a particular deposition zone, transport distance, or particle-size mechanism. Reviews of metal-bearing atmospheric particulate matter identify possible airborne pathways [45]. Remote sensing has been used to monitor mining environments [46] and to investigate soil and vegetation metal signals [47], but neither approach substitutes for measured concentration–distance profiles at Temirtau.

Distance correlations for some elements were weaker than those for others. This observation is compatible with spatial heterogeneity but does not identify atmospheric circulation, topographic trapping, or element-specific mobility as the cause. Distances must be defined relative to specific sources, and potentially confounding variables must be considered before mechanistic conclusions are drawn.

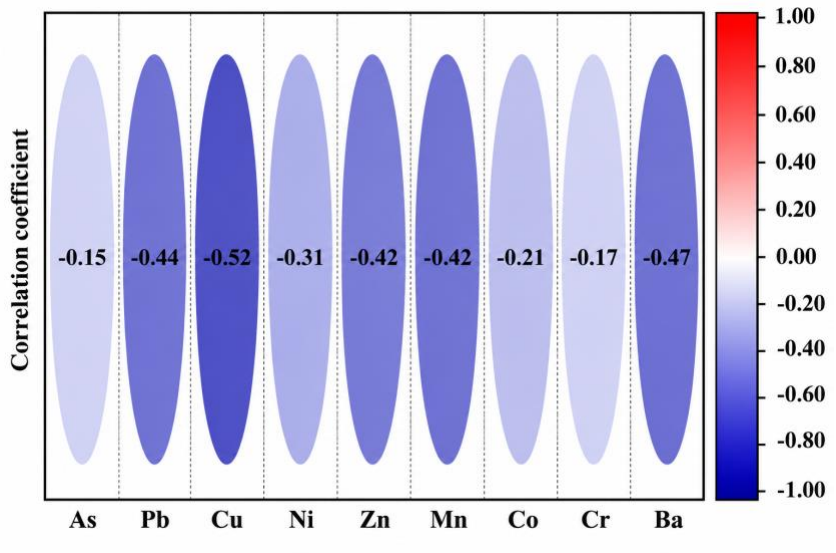

Figure 3. Reported correlations between distance from industrial facilities and concentrations of the nine elements. The plot shows correlation coefficients, not measured concentration–distance profiles or buffer-zone means.

Figure 4 summarizes selected pairwise Pearson correlations among the measured element concentrations. The strongest reported positive correlation was between Mn and Cu ($r = 0.64$; reported $p = 0.0005$). Positive correlations were also reported for Mn–Zn, Zn–Cr, and Zn–Ba, but the exact p-values and any multiple-testing adjustment are not provided. Nine elements permit 36 distinct pairwise tests, so statistical significance should be interpreted with attention to multiple comparisons.

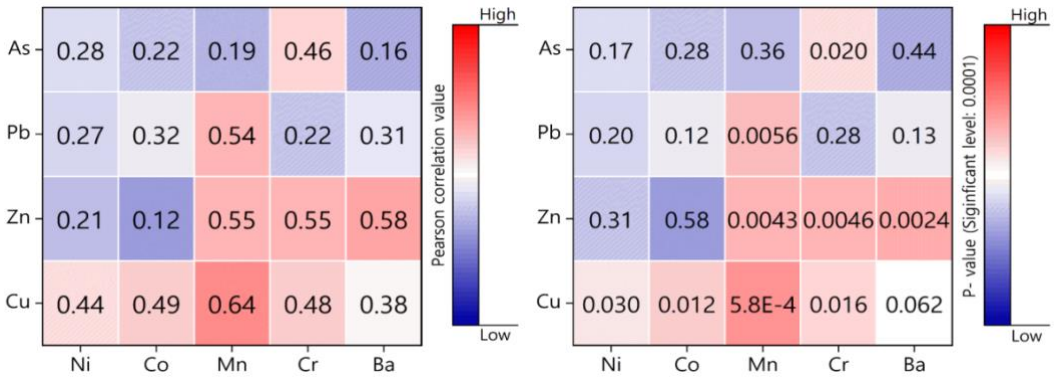

Figure 4. DBE–carbon number distribution of O_2-class compounds in Beke bitumen.

Inter-element correlation indicates co-variation rather than a shared emission source or chemical interaction. Studies have combined geostatistics with Moran's I to examine spatial clustering of soil metals

© 2026 Jusan Science Publisher LTD. All rights reserved.
This is an open access article distributed under the terms of the Creative Commons Attribution (CC BY 4.0) license.

[48], and receptor–geostatistical models have been used to investigate potential source contributions [49]. Because spatial autocorrelation and source heterogeneity were not evaluated here, the observed associations are hypotheses for further investigation, not confirmation of common industrial origins.

Regression fits were compared for selected element pairs (Table 1; Figure 5). Some nonlinear functions achieved higher in-sample R^2 values than linear models, including the reported cubic Zn–Cr model ($R^2 = 0.79$). However, adding polynomial terms can improve in-sample fit even when the underlying relationship is not reproducible. With only 25 sampling locations and no reported validation or residual analysis, the apparent nonlinear patterns should not be treated as robust evidence of nonlinear geochemical transport mechanisms.

Table 1. Reported in-sample regression-fit statistics for selected element pairs. Values and equations have not been independently recalculated; see the table note and author-verification list.

Model	Function	Reported fit statistic*	Coefficient of Determination (R^2)	Mean Approximation Error (%)
Pb and Mn				
Linear	$y = 9.2142x + 3011.9581$	0.5378	0.2893	17.03
Quadratic	$y = -0.0055x^2 + 10.0754x + 2996.9958$	0.5381	0.2895	16.99
Cubic	$y = -0.0000x^3 - 0.0001x^2 + 9.7351x + 2999.2416$	0.5381	0.2896	16.99
Exponential	$y = 2991.6932 \cdot 1.0024^x$	0.5275	0.2783	16.43
Zn and Mn				
Linear	$y = 0.67x + 3077.94$	0.55	0.30	18.13
Quadratic	$y = -0.00x^2 + 3.72x + 1658.56$	0.74	0.50	15.63
Cubic	$y = -0.00x^3 + 0.00x^2 + 1.34x + 2428.04$	0.77	0.59	14.74
Power	$y = 617.25x^{0.27}$	0.63	0.40	15.92
Exponential	$y = 3068.13 \cdot 1.00^x$	0.51	0.26	17.79
Logarithmic	$y = -3232.14 + 1064.08 \cdot \ln x$	0.66	0.44	16.30
Exponential Form	$y = e^{8.03} + 0.00x$	0.51	0.26	17.79
Cu and Mn				
Linear	$y = 7.28x + 1884.82$	0.64	0.41	16.14
Quadratic	$y = -0.01x^2 + 14.21x + 937.69$	0.65	0.42	16.28
Cubic	$y = -0.00x^3 + 0.31x^2 - 80.02x + 9391.54$	0.70	0.49	15.07
Power	$y = 197.64x^{0.53}$	0.64	0.41	15.71
Exponential	$y = 2255.35 \cdot 1.00^x$	0.61	0.38	16.01
Logarithmic	$y = -7547.25 + 2059.24 \cdot \ln x$	0.64	0.41	16.42
Hyperbolic	$y = 5904.21 - 496232.12/x$	0.62	0.39	16.77
Exponential Form	$y = e^{7.72} + 0.00x$	0.61	0.38	16.01
Zn and Cr				
Linear	$y = 0.25x + 195.43$	0.55	0.30	34.02
Cubic	$y = -0.00x^3 + 0.00x^2 - 2.19x + 907.01$	0.89	0.79	27.54
Power	$y = 31.54x0.37$	0.45	0.20	24.62
Exponential	$y = 272.19 \cdot 1.00^x$	0.43	0.19	24.09
Exponential Form	$y = e5.61 + 0.00x$	0.43	0.19	24.09
Zn and Ba				
Linear	$y = 0.46x + 1867.04$	0.58	0.34	16.00
Power	$y = 406.17x0.26$	0.60	0.36	15.41
Exponential	$y = 1862.06 \cdot 1.00^x$	0.56	0.31	15.32
Exponential Form	$y = e7.53 + 0.00x$	0.56	0.31	15.32

For Zn–Cr, the cubic fit had the highest reported in-sample R^2 (0.79), but its reported mean approximation error (27.54%) exceeded that of the power-law (24.62%) and exponential (24.09%) alternatives. Therefore, the cubic model cannot be called the unambiguously 'best' model without a predefined selection criterion and out-of-sample comparison. Several fitted equations include coefficients rounded to 0.00 or 1.00, which makes them impossible to reproduce reliably. In addition, the Zn–Mn quadratic row reports a fit statistic of 0.74 and $R^2 = 0.50$; if the former is intended as the nonnegative square root of R^2, these values are inconsistent ($0.74^2 \approx 0.55$).

© 2026 Jusan Science Publisher LTD. All rights reserved.
This is an open access article distributed under the terms of the Creative Commons Attribution (CC BY 4.0) license.

https://doi.org/10.66973/jees.26.012

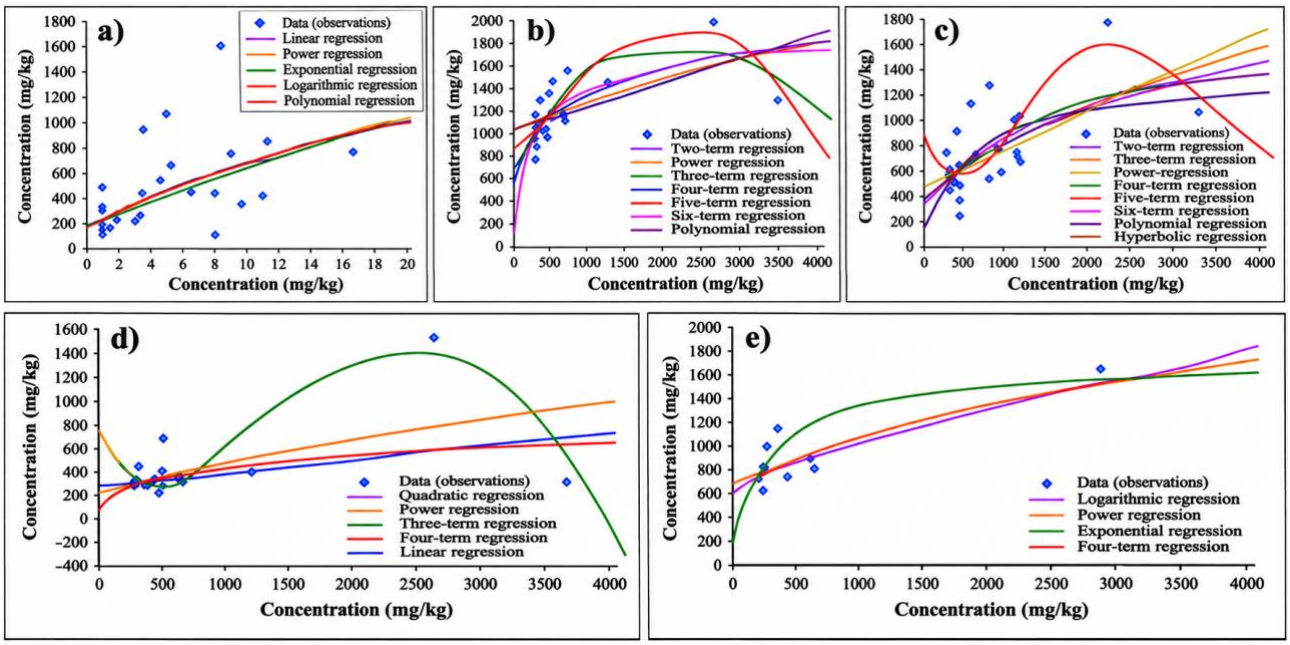

Figure 5. In-sample regression curves for selected element pairs: (a) Pb–Mn; (b) Zn–Mn; (c) Cu–Mn; (d) Zn–Cr; and (e) Zn–Ba. The curves are descriptive fits and have not been validated for prediction.

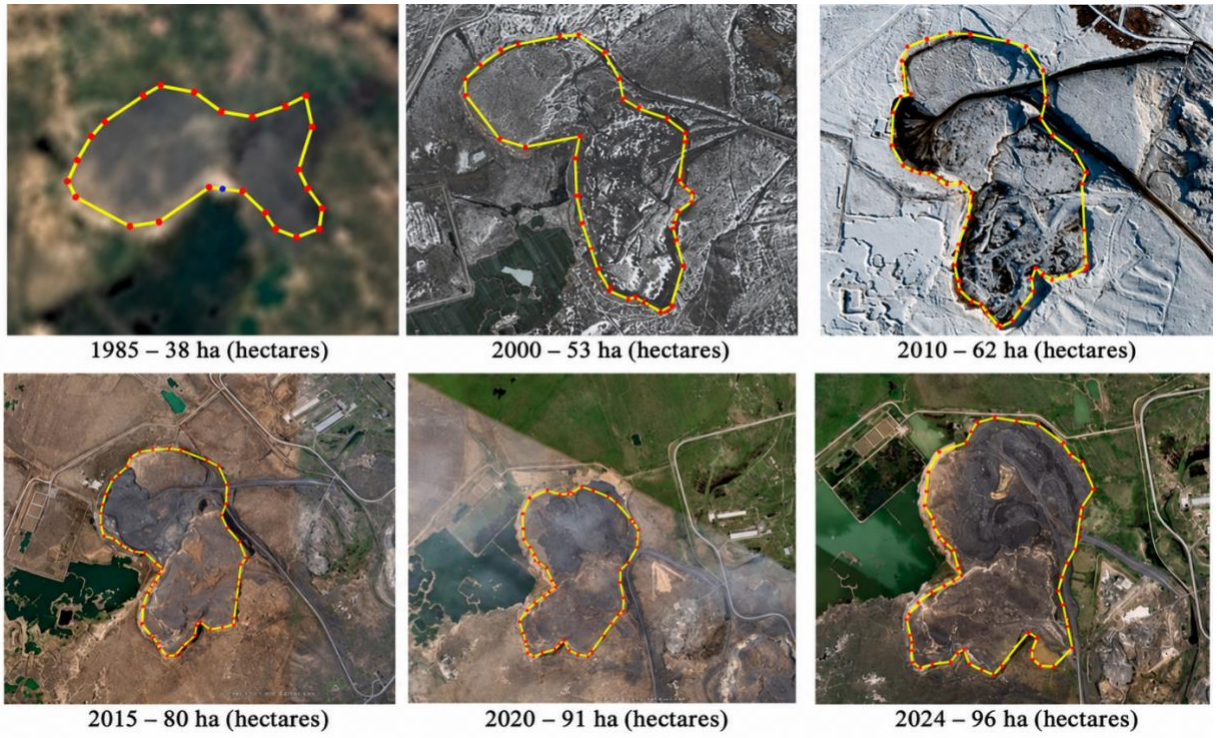

Figure 6. Mapped area of industrial waste deposits from 1985 to 2024: 1985, 38 ha; 2000, 53 ha; 2010, 62 ha; 2015, 80 ha; 2020, 91 ha; and 2024, 96 ha.

The remotely mapped area of industrial waste deposits increased from 38 ha in 1985 to 96 ha in 2024 (Figure 6), corresponding to 58 ha of additional mapped area (approximately 153%) and a 2.53-fold final-to-initial

© 2026 Jusan Science Publisher LTD. All rights reserved.
This is an open access article distributed under the terms of the Creative Commons Attribution (CC BY 4.0) license.

ratio. Regional studies of surface-water change [50] and glacier dynamics [51] illustrate the use of multi-date geospatial observations for environmental monitoring, but do not validate the waste-area boundaries in this study. Spectral estimation of soil metals has been investigated in mining-reclamation settings [52]; it requires calibration and is distinct from delineating waste-deposit area on satellite imagery. Formal source-specific health-risk assessment also requires explicit source and uncertainty modeling [53]. Smelting-related deposition [54] and pollutant-bearing road dust [55] are pathways documented elsewhere, not mechanisms measured by these images. The mapped area estimates depend on imagery, boundary delineation, and classification accuracy, none of which was reported sufficiently for independent verification. The images cannot directly establish changes in soil-metal concentrations or a causal relationship between waste-area expansion and metal migration.

Figure 7 shows the reported ArcGIS ModelBuilder workflow. The manuscript lists distance, terrain slope, NDVI, soil pH, nitrogen content, and organic carbon as spatial inputs, but does not provide the actual numerical weights or an independently reproducible overlay equation. Furthermore, the Methods describe equal weighting while the Results invoke correlation-based weighting. This inconsistency prevents a defensible ranking of the influence of individual factors.

The integrated GIS maps show spatial variation in the calculated composite scores. Because these scores combine measured/interpolated concentrations with reclassified contextual layers, they must not be treated as independently measured metal concentrations. Claims that distance 'dominates' Pb, Cu, Zn, and Mn distributions, or that NDVI and pH exert significant independent effects, are not supported without explicit weights, uncertainty analysis, and a model that can distinguish association from causation.

The nine composite maps in Figure 8 represent the results of the stated GIS overlay for the available inputs. They do not provide forecasts of future metal concentrations because no time-dependent emissions, transport, or concentration model was developed or validated. Nor do they quantify ecological or human-health risk: such conclusions would require relevant exposure assumptions, toxicological benchmarks, or an established risk-index calculation.

The composite maps may help identify locations for additional soil sampling, but their usefulness for management decisions remains conditional on analytical quality control, reproducible raster processing, interpolation validation, and comparison with relevant background concentrations or soil-quality standards. Without these steps, high composite scores should be described as monitoring priorities rather than confirmed hazardous zones.

Taken together, the reported maps and statistical analyses suggest element-specific spatial heterogeneity and some co-variation in the 25 sampled soils. The data do not independently identify contamination sources, prove transport mechanisms, quantify ecological or human-health risk, or support future-concentration forecasts. These distinctions are essential for interpreting the results without overstating their evidential strength.

Study Limitations

This exploratory study is limited by its small, non-randomly described sampling network (n = 25), incomplete reporting of XRF quality control and concentration distributions, and absence of interpolation cross-validation or prediction-uncertainty estimates. The manuscript also lacks a reproducible specification of the integrated GIS weights and raster inputs. These limitations restrict the spatial generalizability and reproducibility of the maps.

Pairwise correlations and flexible regression curves are descriptive and do not establish source attribution, causal mechanisms, or predictive performance. The reported regression equations require full-precision coefficients and independent model checks. Finally, the study does not present a formal background-based contamination assessment or an exposure-based risk assessment; its composite maps cannot substitute for either.

© 2026 Jusan Science Publisher LTD. All rights reserved.
This is an open access article distributed under the terms of the Creative Commons Attribution (CC BY 4.0) license.

https://doi.org/10.66973/jees.26.012



Figure 7. ArcGIS ModelBuilder workflow used to combine reclassified spatial layers into element-specific integrated maps.

© 2026 Jusan Science Publisher LTD. All rights reserved.
This is an open access article distributed under the terms of the Creative Commons Attribution (CC BY 4.0) license.

https://doi.org/10.66973/jees.26.012

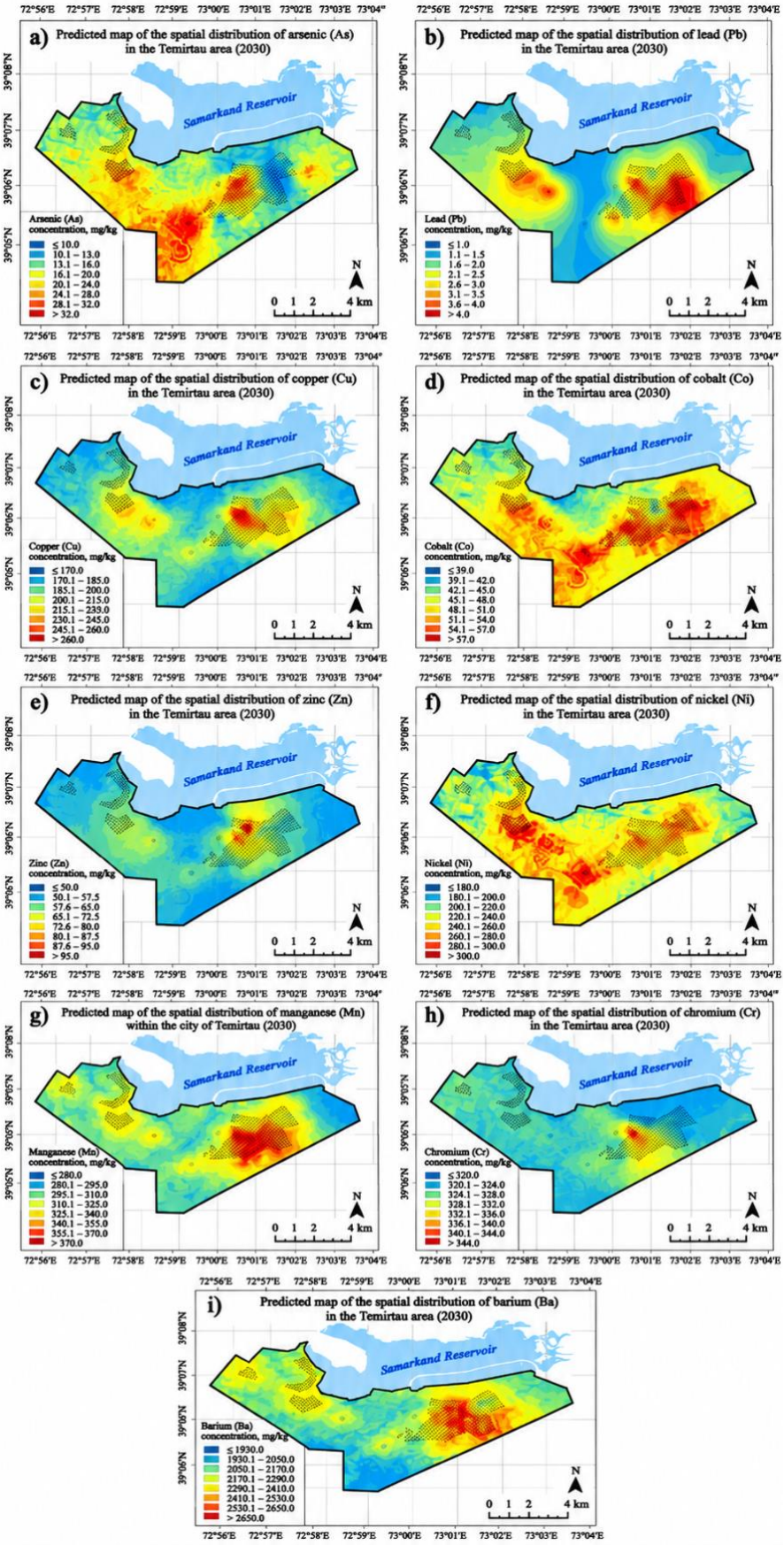

Figure 8. Element-specific composite spatial indicators from the ArcGIS overlay for (a) As; (b) Pb; (c) Cu; (d) Co; (e) Zn; (f) Ni; (g) Mn; (h) Cr; and (i) Ba. These are exploratory modeled surfaces, not validated temporal forecasts or quantitative risk maps.

© 2026 Jusan Science Publisher LTD. All rights reserved.
This is an open access article distributed under the terms of the Creative Commons Attribution (CC BY 4.0) license.

https://doi.org/10.66973/jees.26.012

4 Conclusion

This study combined XRF measurements from 25 surface-soil samples with GIS interpolation and statistical analyses to describe nine potentially toxic elements in the Temirtau industrial area. The interpolated surfaces suggested localized areas of relatively elevated Pb, Zn, Cu, Mn, Ba, and Cr concentrations, while As, Ni, and Co appeared more spatially dispersed. These findings describe the sampled area but require interpolation validation before being generalized to unsampled locations.

The strongest reported inter-element Pearson correlation was Mn–Cu ($r = 0.64$; reported $p = 0.0005$). Additional positive associations were reported for Mn–Zn, Zn–Cr, and Zn–Ba. These observations indicate statistical co-variation, not confirmed shared industrial sources or element migration mechanisms; complete p-values and an appropriate multiple-testing strategy remain to be reported.

The cubic Zn–Cr regression yielded a reported in-sample R^2 of 0.79, but alternative functions had lower reported approximation errors. No model can be designated reliably as superior until the error metric is defined, coefficients are reported precisely, and out-of-sample validation and residual diagnostics are provided.

The mapped area of industrial waste deposits increased from 38 ha in 1985 to 96 ha in 2024 (58 ha; approximately 153% increase). This is evidence of mapped areal expansion, not direct evidence of increased metal mobility or environmental exposure. The ArcGIS ModelBuilder workflow produced nine composite spatial indicators. Because its weighting scheme is described inconsistently and the workflow was not independently validated, the resulting maps should not be presented as forecasts of future concentrations or quantitative environmental-risk maps. Complete model settings, analytical quality control, and spatial validation are prerequisites for stronger applications.

Overall, the study provides preliminary spatial evidence that may guide targeted monitoring and hypothesis development. Further sampling, complete concentration and quality-control reporting, validated spatial models, and appropriately designed source or risk assessments are needed before drawing firm conclusions about contamination sources, hazards, or future trends.

The contribution of the work is therefore an exploratory integration of field measurements, geostatistical maps, and descriptive statistical associations—not a validated predictive model of contaminant transport.

Funding

This research received no external funding.

Author Contributions

M.A.: Investigation, data collection, methodology, and original draft preparation; Y.Z.: Conceptualization, supervision, methodology, and writing—review and editing; Y.B.: GIS analysis, spatial modeling, visualization, and validation; A.A.: Investigation, laboratory analysis, and data curation; A.T.: Statistical analysis, data interpretation, and visualization; Y.A.: Data processing, formal analysis, and manuscript review.

Ethics Approval and Consent to Participate

This study did not involve human participants or animals. Therefore, ethical approval and informed consent were not required.

Data Availability Statement

The data supporting the findings of this study are available from the corresponding author upon reasonable request.

Supporting Information

Not applicable.

Conflict of Interest

The authors declare no conflict of interest.

AI Use Disclosure

No AI tools were used to generate scientific results, data, figures, or interpretations. All analyses, conclusions, and scientific content were developed by the authors.

© 2026 Jusan Science Publisher LTD. All rights reserved.
This is an open access article distributed under the terms of the Creative Commons Attribution (CC BY 4.0) license.

REFERENCES

[1] T. Zhang, W. Xu, X. Lin, H. Yan, M. Ma, and Z. He, "Assessment of heavy metals pollution of soybean grains in North Anhui of China," *Science of the Total Environment*, vol. 646, pp. 914–922, 2019. https://doi.org/10.1016/j.scitotenv.2018.07.335
[2] S. Islam, K. Ahmed, Habibullah-Al-Mamun, and S. Masunaga, "Potential ecological risk of hazardous elements in different land-use urban soils of Bangladesh," *Science of the Total Environment*, vols. 512–513, pp. 94–102, 2015. https://doi.org/10.1016/j.scitotenv.2014.12.100
[3] M. Amirkhanov, Y. Zhakypbek, S. Tursbekov, and T. Nurpeissova, "Comparative analysis of the state of desertification of the lands of West and East Kazakhstan," *Engineering Journal of Satbayev University*, vol. 147, no. 2, pp. 40–49, 2025. https://doi.org/10.51301/ejsu.2025.i2.06
[4] D. Hou, D. O'Connor, P. Nathanail, L. Tian, and Y. Ma, "Integrated GIS and multivariate statistical analysis for regional-scale assessment of heavy metal soil contamination: A critical review," *Environmental Pollution*, vol. 231, pp. 1188–1200, 2017. https://doi.org/10.1016/j.envpol.2017.07.021
[5] M. A. Mukasheva, G. Zh. Mukasheva, D. V. Surzhikov, A. K. Arymbekova, and B. Zernke, "Status of soil cover on the degree of accumulation of heavy metals in the soil of the industrial region (Karaganda city)," *Fundamental and Experimental Biology*, vol. 85, no. 1, pp. 9–14, 2017. https://doi.org/10.31489/2017bmg1/9-14
[6] R. Salimbayeva, T. Randhir, K. Stamkulova, A. Daulbayeva, G. Satbaeva, Z. Yessenkulova, and Z. Moldagazyyeva, "Integrated assessment of air, soil, and water pollution in the Karaganda region of Central Kazakhstan: Hotspots, salinization, and ecological risks," *Brazilian Journal of Biology*, vol. 86, Art. no. e301405, 2026. https://doi.org/10.1590/1519-6984.301405
[7] Y. Tseshkovskaya, N. Tsoy, V. Tseshkovskiy, M. Ibrayev, N. Zamaliyev, D. Akhmatnurov, R. Mussin, N. Ganyukov, A. Zakharov, K. Skrzypkowski, *et al*., "Research progress of environmental studies of a mining facility for land restoration (using the example of a mining enterprise in the Karaganda region)," *Resources*, vol. 14, no. 9, Art. no. 144, 2025. https://doi.org/10.3390/resources14090144
[8] J. P. Vareda, A. J. M. Valente, and L. Durães, "Assessment of heavy metal pollution from anthropogenic activities and remediation strategies: A review," *Journal of Environmental Management*, vol. 246, pp. 101–118, 2019. https://doi.org/10.1016/j.jenvman.2019.05.126
[9] O. Enya, C. Lin, and J. Qin, "Heavy metal contamination status in soil-plant system in the Upper Mersey Estuarine Floodplain, Northwest England," *Marine Pollution Bulletin*, vol. 146, pp. 292–304, 2019. https://doi.org/10.1016/j.marpolbul.2019.06.026
[10] M. Gope, R. E. Masto, J. George, R. R. Hoque, and S. Balachandran, "Bioavailability and health risk of some potentially toxic elements (Cd, Cu, Pb and Zn) in street dust of Asansol, India," *Ecotoxicology and Environmental Safety*, vol. 138, pp. 231–241, 2017. https://doi.org/10.1016/j.ecoenv.2017.01.008
[11] R. Sun, Y. Gao, and Y. Yang, "Leaching of heavy metals from lead–zinc mine tailings and the subsequent migration and transformation characteristics in paddy soil," *Chemosphere*, vol. 291, Art. no. 132792, 2022. https://doi.org/10.1016/j.chemosphere.2021.132792
[12] C. Zhang, Z. Li, W. Yang, L. Pan, M. Gu, and D. Lee, "Assessment of metals pollution on agricultural soil surrounding a lead–zinc mining area in the karst region of Guangxi, China," *Bulletin of Environmental Contamination and Toxicology*, vol. 90, no. 6, pp. 736–741, 2013. https://doi.org/10.1007/s00128-013-0987-6
[13] Y. Ma, X. Yao, J. Wang, H. Duan, J. Hu, and T. Wu, "Characteristics and sources of heavy metal pollution in cropland near a typical lead-zinc processing plant in Xieping Village, Hui County, China," *Land*, vol. 12, no. 10, Art. no. 1945, 2023. https://doi.org/10.3390/land12101945
[14] Z. Wu, H. Li, L. Lu, G. Liang, T. Wu, and J. Zhu, "Distributions and risk assessment of heavy metals in solid waste in lead–zinc mining areas and across the soil, water body, sediment and agricultural product ecosystem in their surrounding areas," *China Geology*, vol. 8, no. 1, pp. 92–106, 2025. https://doi.org/10.31035/cg2024036
[15] J. Cao, C. Xie, and Z. Hou, "Ecological evaluation of heavy metal pollution in the soil of Pb–Zn mines," *Ecotoxicology*, vol. 31, pp. 259–270, 2022. https://doi.org/10.1007/s10646-021-02505-3
[16] S. Zhang, Y. Liu, Y. Yang, X. Ni, A. Muhammad, C. Wokadala, and C. Li, "Trace elements in soils of a typical industrial district in Ningxia, Northwest China: Pollution, source, and risk evaluation," *Sustainability*, vol. 12, no. 5, Art. no. 1868, 2020. https://doi.org/10.3390/su12051868
[17] Y. Gao, F. Chen, H. Zhang, and Z. Wang, "Pollution and health risk assessment of heavy metals in soils of Guizhou, China," *Ecosystem Health and Sustainability*, vol. 7, no. 1, Art. no. 1859948, 2021. https://doi.org/10.1080/20964129.2020.1859948
[18] W. Ding, C. Lv, J. Xi, *et al*., "Assessment of heavy metal pollution and risks in mining soils in China," *Environment, Development and Sustainability*, 2026. https://doi.org/10.1007/s10668-026-08243-y
[19] R. Liu, Y. Xu, J. Zhang, H. Chen, F. He, G. Qiao, H. Ke, and Y. Shi, "A comparative study of the content of heavy metals in typical metallic mine rivers of the Tibetan Plateau," *Geological Bulletin of China*, vol. 37, no. 12, pp. 2154–2168, 2018. https://doi.org/10.12097/j.issn.1671-2552.2018.12.005
[20] X. Nan, H. Zhang, and C. Shi, "Study on health evaluation of cultivated land in mining area," *China Mining Magazine*, vol. 30, no. 10, pp. 66–70, 2021. https://dx.doi.org/10.12075/j.issn.1004-4051.2021.10.025.

© 2026 Jusan Science Publisher LTD. All rights reserved.
This is an open access article distributed under the terms of the Creative Commons Attribution (CC BY 4.0) license.

[21] X. Zhu, B. Xue, X. Li, J. Wang, X. Shang, C. Chen, P. Geng, Z. Kou, and X. Ma, "Sources apportionment of heavy metals in farmland soil around lead–zinc tailings reservoir based on PMF model," *Journal of Northwest University (Natural Science Edition)*, vol. 51, no. 1, pp. 43–53, 2021. https://doi.org/10.16152/j.cnki.xdxbzr.2021-01-006.
[22] Z. Bai, W. Zhou, J. Wang, Z. Zhao, Y. Cao, and Y. Zhou, "Rethink on ecosystem restoration and rehabilitation of mining areas," *China Land Science*, vol. 32, no. 11, pp. 1–9, 2018. https://doi.org/10.11994/zgtdkx.20181107.162318
[23] Z. Bai, "The major issues in ecological restoration of China's territorial space," *Earth Science Frontiers*, vol. 28, no. 4, pp. 1–13, 2021. https://doi.org/10.13745/j.esf.sf.2021.6.20
[24] S. Li, Z. Dan, and T. Yin, "Mining-induced land use change and ecological restoration: Lessons from three developing economies," *Physics and Chemistry of the Earth, Parts A/B/C*, Art. no. 104267, 2025. https://doi.org/10.1016/j.pce.2025.104267
[25] Q. Zhang, G. Han, M. Liu, X. Li, L. Wang, and B. Liang, "Distribution and contamination assessment of soil heavy metals in the Jiulongjiang River catchment, Southeast China," *International Journal of Environmental Research and Public Health*, vol. 16, no. 23, Art. no. 4674, 2019. https://doi.org/10.3390/ijerph16234674
[26] J. Wang, C. Dong, S. Sun, L. Mu, N. Zhang, and L. Bao, "Characteristics and correlation analysis of the spatial distribution of heavy metals in arable soils with different soil-forming matrices," *Sustainability*, vol. 16, no. 23, Art. no. 10338, 2024. https://doi.org/10.3390/su162310338
[27] T. Alharbi, S. Almadani, S. Shoaib, N. Rikan, J. Meroño, and M. Shokr, "An integrated GIS–statistical approach to assess soil contamination in Al-Muzahmiya, Saudi Arabia: Implications for food security," *Frontiers in Sustainable Food Systems*, vol. 9, Art. no. 1695962, 2025. https://doi.org/10.3389/fsufs.2025.1695962
[28] S. Dragović, N. Mihailović, and B. Gajić, "Heavy metals in soils: Distribution, relationship with soil characteristics and radionuclides and multivariate assessment of contamination sources," *Chemosphere*, vol. 72, no. 3, pp. 491–495, 2008. https://doi.org/10.1016/j.chemosphere.2008.02.063
[29] X. J. Wang, Y. Zheng, R. M. Liu, B. G. Li, J. Cao, and S. Tao, "Kriging and PAH pollution assessment in the topsoil of Tianjin area," *Bulletin of Environmental Contamination and Toxicology*, vol. 71, no. 1, pp. 189–195, 2003. https://doi.org/10.1007/s00128-003-0148-4
[30] L. Fabri, A. Kuznetsov, N. Rollo, and P. Fattal, "Natural degradation of spilt fuel oil on seacoasts: Modelling, mapping, and spatial analysis," *Regional Studies in Marine Science*, vol. 58, Art. no. 102782, 2023. https://doi.org/10.1016/j.rsma.2022.102782
[31] A. Aitimbetova and Z. Pernebayev, "Municipal solid waste in Shymkent: Environmental impact and management approaches," *Sustainability*, vol. 18, no. 6, Art. no. 2745, 2026. https://doi.org/10.3390/su18062745
[32] S. Heaven, M. A. Ilyushchenko, I. M. Kamberov, M. I. Politikov, T. W. Tanton, S. M. Ullrich, and E. P. Yanin, "Mercury in the River Nura and its floodplain, Central Kazakhstan: II. Floodplain soils and riverbank silt deposits," *Science of the Total Environment*, vol. 260, pp. 45–55, 2000. https://doi.org/10.1016/S0048-9697(00)00566-0
[33] A. Facchinelli, E. Sacchi, and L. Mallen, "Multivariate statistical and GIS-based approach to identify heavy metal sources in soils," *Environmental Pollution*, vol. 114, pp. 313–324, 2001. https://doi.org/10.1016/S0269-7491(00)00243-8
[34] P. Goovaerts, *Geostatistics for Natural Resources Evaluation*. New York, NY, USA: Oxford University Press, 1997. https://doi.org/10.1093/oso/9780195115383.001.0001
[35] Y. Xie, T. B. Chen, M. Lei, J. Yang, Q. J. Guo, B. Song, and X. Y. Zhou, "Spatial distribution of soil heavy metal pollution estimated by different interpolation methods: Accuracy and uncertainty analysis," *Chemosphere*, vol. 82, pp. 468–476, 2011. https://doi.org/10.1016/j.chemosphere.2010.09.053
[36] M. Amirkhanov, Y. Zhakypbek, and S. Hao, "Geospatial model for land degradation assessment in the Caspian region based on integrated multifactor indicators," *Engineering Journal of Satbayev University*, vol. 148, no. 3, pp. 24–32, 2026. https://doi.org/10.51301/ejsu.2026.i3.04
[37] C. Qu, W. Chen, X. Hu, P. Cai, C. Chen, X. Y. Yu, and Q. Huang, "Heavy metal behaviour at mineral-organo interfaces: Mechanisms, modelling and influence factors," *Environment International*, vol. 131, Art. no. 104995, 2019. https://doi.org/10.1016/j.envint.2019.104995
[38] Q. Li, Y. Wang, Y. Li, L. Li, M. Tang, W. Hu, L. Chen, and S. Ai, "Speciation of heavy metals in soils and their immobilization at micro-scale interfaces among diverse soil components," *Science of the Total Environment*, vol. 825, Art. no. 153862, 2022. https://doi.org/10.1016/j.scitotenv.2022.153862
[39] J. Pérez-Esteban, C. Escolástico, A. Masaguer, C. Vargas, and A. Moliner, "Soluble organic carbon and pH of organic amendments affect metal mobility and chemical speciation in mine soils," *Chemosphere*, vol. 103, pp. 164–171, 2014. https://doi.org/10.1016/j.chemosphere.2013.11.055
[40] L. Qiu, K. Wang, W. Long, K. Wang, W. Hu, and G. S. Amable, "A comparative assessment of the influences of human impacts on soil Cd concentrations based on stepwise linear regression, classification and regression tree, and random forest models," *PLOS ONE*, vol. 11, no. 3, Art. no. e0151131, 2016. https://doi.org/10.1371/journal.pone.0151131
[41] X. Xiao, J. Zhang, H. Wang, X. Han, J. Ma, Y. Ma, and H. Luan, "Distribution and health risk assessment of potentially toxic elements in soils around coal industrial areas: A global meta-analysis," *Science of the Total Environment*, vol. 713, Art. no. 135292, 2020. https://doi.org/10.1016/j.scitotenv.2019.135292

© 2026 Jusan Science Publisher LTD. All rights reserved.
This is an open access article distributed under the terms of the Creative Commons Attribution (CC BY 4.0) license.

[42] Y. Song, L. Kang, F. Lin, N. Sun, A. Aizezi, Z. Yang, and X. Wu, "Estimating the spatial distribution of soil heavy metals in oil mining area using air quality data," *Atmospheric Environment*, vol. 287, Art. no. 119274, 2022. https://doi.org/10.1016/j.atmosenv.2022.119274
[43] P. Liu, Q. Wu, W. Hu, K. Tian, B. Huang, and Y. Zhao, "Effects of atmospheric deposition on heavy metals accumulation in agricultural soils: Evidence from field monitoring and Pb isotope analysis," *Environmental Pollution*, vol. 330, Art. no. 121740, 2023. https://doi.org/10.1016/j.envpol.2023.121740
[44] Z. Adamczyk and K. Nowińska, "Environmental mobility of trace elements present in dusts emitted from Zn–Pb metallurgical processes," *Environmental Earth Sciences*, vol. 75, Art. no. 956, 2016. https://doi.org/10.1007/s12665-016-5765-4
[45] L. T. Popoola, S. A. Adebanjo, and B. K. Adeoye, "Assessment of atmospheric particulate matter and heavy metals: A critical review," *International Journal of Environmental Science and Technology*, vol. 15, pp. 935–948, 2018. https://doi.org/10.1007/s13762-017-1454-4
[46] W. Song, W. Song, H. Gu, and F. Li, "Progress in the remote sensing monitoring of the ecological environment in mining areas," *International Journal of Environmental Research and Public Health*, vol. 17, no. 6, Art. no. 1846, 2020. https://doi.org/10.3390/ijerph17061846
[47] V. Lovynska, B. Bayat, R. Bol, S. Moradi, M. Rahmati, R. Raj, S. Sytnyk, O. Wiche, B. Wu, and C. Montzka, "Monitoring heavy metals and metalloids in soils and vegetation by remote sensing: A review," *Remote Sensing*, vol. 16, no. 17, Art. no. 3221, 2024. https://doi.org/10.3390/rs16173221
[48] X. N. Huo, H. Li, D. F. Sun, L. D. Zhou, and B. G. Li, "Combining geostatistics with Moran's I analysis for mapping soil heavy metals in Beijing, China," *International Journal of Environmental Research and Public Health*, vol. 9, no. 3, pp. 995–1017, 2012. https://doi.org/10.3390/ijerph9030995
[49] Z. Wang, X. Chen, D. Yu, L. Zhang, J. Wang, and J. Lv, "Source apportionment and spatial distribution of potentially toxic elements in soils: A new exploration on receptor and geostatistical models," *Science of the Total Environment*, vol. 759, Art. no. 143428, 2021. https://doi.org/10.1016/j.scitotenv.2020.143428
[50] M. Amirkhanov, Y. Zhakypbek, N. Mukhambetzhanova, and S. Hao, "Spatial and temporal analysis of the dynamics of surface water changes in Makat and Zhylyoi districts," *Mining Journal of Kazakhstan*, no. 8, pp. 31–38, 2026. https://doi.org/10.48498/minmag.2026.256.8.008
[51] M. Amirkhanov, Y. Zhakypbek, A. Aben, and N. Mussakhan, "Monitoring of glaciation and melting in the East Kazakhstan region," *Mining Journal of Kazakhstan*, no. 11, pp. 27–32, 2023. https://doi.org/10.48498/minmag.2023.223.11.007
[52] J. Dong, W. Dai, J. Xu, and S. Li, "Spectral estimation model construction of heavy metals in mining reclamation areas," *International Journal of Environmental Research and Public Health*, vol. 13, no. 7, Art. no. 640, 2016. https://doi.org/10.3390/ijerph13070640
[53] M. Lei, K. Li, G. Guo, and T. Ju, "Source-specific health risks apportionment of soil potential toxicity elements combining multiple receptor models with Monte Carlo simulation," *Science of the Total Environment*, vol. 817, Art. no. 152899, 2022. https://doi.org/10.1016/j.scitotenv.2021.152899
[54] E. Yu, H. Liu, Y. Tu, X. Gu, X. Ran, Z. Yu, and P. Wu, "Superposition effects of zinc smelting atmospheric deposition on soil heavy metal pollution under geochemical anomaly," *Frontiers in Environmental Science*, vol. 10, Art. no. 777894, 2022. https://doi.org/10.3389/fenvs.2022.777894
[55] D. Vlasov, O. Ramírez, and A. Luhar, "Road dust in urban and industrial environments: Sources, pollutants, impacts, and management," *Atmosphere*, vol. 13, no. 4, Art. no. 607, 2022. https://doi.org/10.3390/atmos13040607

© 2026 Jusan Science Publisher LTD. All rights reserved.
This is an open access article distributed under the terms of the Creative Commons Attribution (CC BY 4.0) license.